40Ar/39Ar mica dating of late Cenozoic sediments in SE Tibet: implications for sediment recycling and drainage evolution

$^{40}Ar/^{39}Ar$ mica dating of late Cenozoic sediments in SE Tibet: implications for sediment recycling and drainage evolution

Xilin Sun[1,2,3]*, K. F. Kuiper[2], Yuntao Tian[1], Chang'an Li[3], Zengjie Zhang[1,4], L. Gemignani[2,5], Rujun Guo[3], Vincent, H.L. de Breij [2] and J. R. Wijbrans[2]

[1] School of Earth Sciences and Engineering, Sun Yat-sen University, Guangzhou 510275, China
[2] Cluster Geology and Geochemistry, Vrije Universiteit Amsterdam, De Boelelaan 1085, 1081 HV Amsterdam, The Netherlands
[3] School of Earth Sciences, China University of Geosciences, Wuhan 430074, China
[4] CAS Key Laboratory of Ocean and Marginal Sea Geology, Guangzhou Institute of Geochemistry, Chinese Academy of Sciences, Guangzhou 510640, China
[5] Department of Earth Science, Freie Universität Berlin, Berlin, 14195 Germany
XS, 0000-0002-6142-5980; ZZ, 0000-0001-7627-9480; LG, 0000-0001-9656-8351
* Correspondence: XS, muscovitesun@gmail.com; CL, chanli@cug.edu.cn

Abstract: The Indo-Asia collision significantly changed the topography and drainage network of rivers around the Tibetan Plateau. Debate continues as to when and how the current drainage system of the Yangtze River was formed. Here we use $^{40}Ar/^{39}Ar$ dating of detrital micas (muscovite and biotite) to constrain provenances of the Pliocene sediments from the Jianchuan and Yuanmou basins in SE Tibet. Muscovite and biotite data of the same Pliocene samples from the Jianchuan Basin suggest contrasting distal v. local sources, respectively. Similarly, muscovite data of the Yuanmou Basin suggest a derivation of sediments from the Yalong River, but the characteristics of the Pliocene cobbles (palaeocurrent and subrounded cobbles) suggest that these sediments are locally sourced. Sediment reworking is proposed as an explanation for the different sediment provenance signals in the Jianchuan and Yuanmou basins that have led to the controversy of an either Pleistocene or pre-Miocene age of formation of the current Yangtze. Based on sediment provenance constraints, the evolution of the Jinsha River is reconstructed. The upper Jinsha River lost its connection with the southward flowing Red River upstream from the Jianchuan basin at least before the Pliocene. At the same time a parallel site in the Yuanmou Basin shows that the Yalong River stopped flowing southward into this basin. Detrital mica from early Pleistocene sediments at the Panzhihua site between the Jianchuan and Yuanmou basins is sourced from the current Jinsha and Yalong rivers. These results would suggest that the current upper Yangtze drainage system should have been established before the Pliocene.

Supplementary material: Muscovite $^{40}Ar/^{39}Ar$ data, biotite $^{40}Ar/^{39}Ar$ data and muscovite geochemistry are available at https://doi.org/10.6084/m9.figshare.c.4821573

Received 11 June 2019; **revised** 12 December 2019; **accepted** 9 January 2020

Uplift of the Tibetan Plateau caused changes in topography and climate, which in turn changed the drainage patterns of rivers in the periphery of the Tibetan Plateau. The eastern and southeastern Tibetan Plateau is drained by three major rivers: the Salween, Mekong and Yangtze rivers (Fig. 1a). The Salween and Mekong rivers flow southwards into the Indian Ocean and South China Sea, respectively. In contrast, headwaters of the Yangtze River, including the Jinsha, Yalong and Dadu rivers, flow southward in the upper reaches and then turn eastward to flow into the East China Sea, as part of the extended Yangtze drainage system (Fig. 1). Previous sediment provenance studies proposed that the Palaeo-Red River catchment was larger than at present and included the present upper Yangtze River and even the Mekong and Salween rivers (Clift *et al.* 2008; Hoang *et al.* 2009; Kong *et al.* 2009, 2012; Yan *et al.* 2012) (Fig. 2). The rivers belonging to the upper Yangtze River originally all flowed southward into the Red River and at some point in time were captured by the middle Yangtze to flow eastward, first into the Sichuan basin and ultimately into the East China Sea (Barbour 1936; Brookfield 1998; Clark *et al.* 2004; Clift *et al.* 2008; Hoang *et al.* 2009; Kong *et al.* 2009, 2012; Yan *et al.* 2012). However, the cause(s) and timing for these capture events remain controversial, with one school of thought proposing early formation of the Yangtze drainage system before the Miocene (Clark *et al.* 2004; Clift *et al.* 2006, 2008; Yan *et al.* 2012; Zheng *et al.* 2013; Wissink *et al.* 2016; Chen *et al.* 2017), and another advocating a Pleistocene capture and formation of the current Yangtze (Yang *et al.* 2006; Kong *et al.* 2009, 2012; Zheng *et al.* 2014).

One way to approach this controversy is to use detrital geochronological methods to unravel sedimentary provenances of Cenozoic sediments deposited in basins along the rivers to reconstruct the palaeo-drainage system for the area. Detrital zircon U–Pb geochronology has been widely used for this purpose (Wissink *et al.* 2016; Chen *et al.* 2017; and references therein). However, no consensus exists on the timing of formation of the current Yangtze River among previous studies using this method (Hoang *et al.* 2009; Kong *et al.* 2009, 2012; Yan *et al.* 2012; Zheng *et al.* 2013; Wissink *et al.* 2016; Chen *et al.* 2017). The controversy may relate to the extremely high durability of zircon to recycling, owing to the high closure temperature of the U–Pb method (>900°C, Lee *et al.* 1997) and zircon's strong resistance to physical and chemical weathering (Hanchar 2013). These characteristics make the detrital zircon U–Pb method less ideal for tracing sediment provenance in areas with polyphase sediment recycling. For example, in the SE of Tibet episodic Mesozoic–Cenozoic orogenic cycles have occurred. It is thus crucial to test whether detrital signals of the Cenozoic deposits in SE Tibet have been influenced by multiple periods of sediment reworking, as this approach could provide important information on the controversy

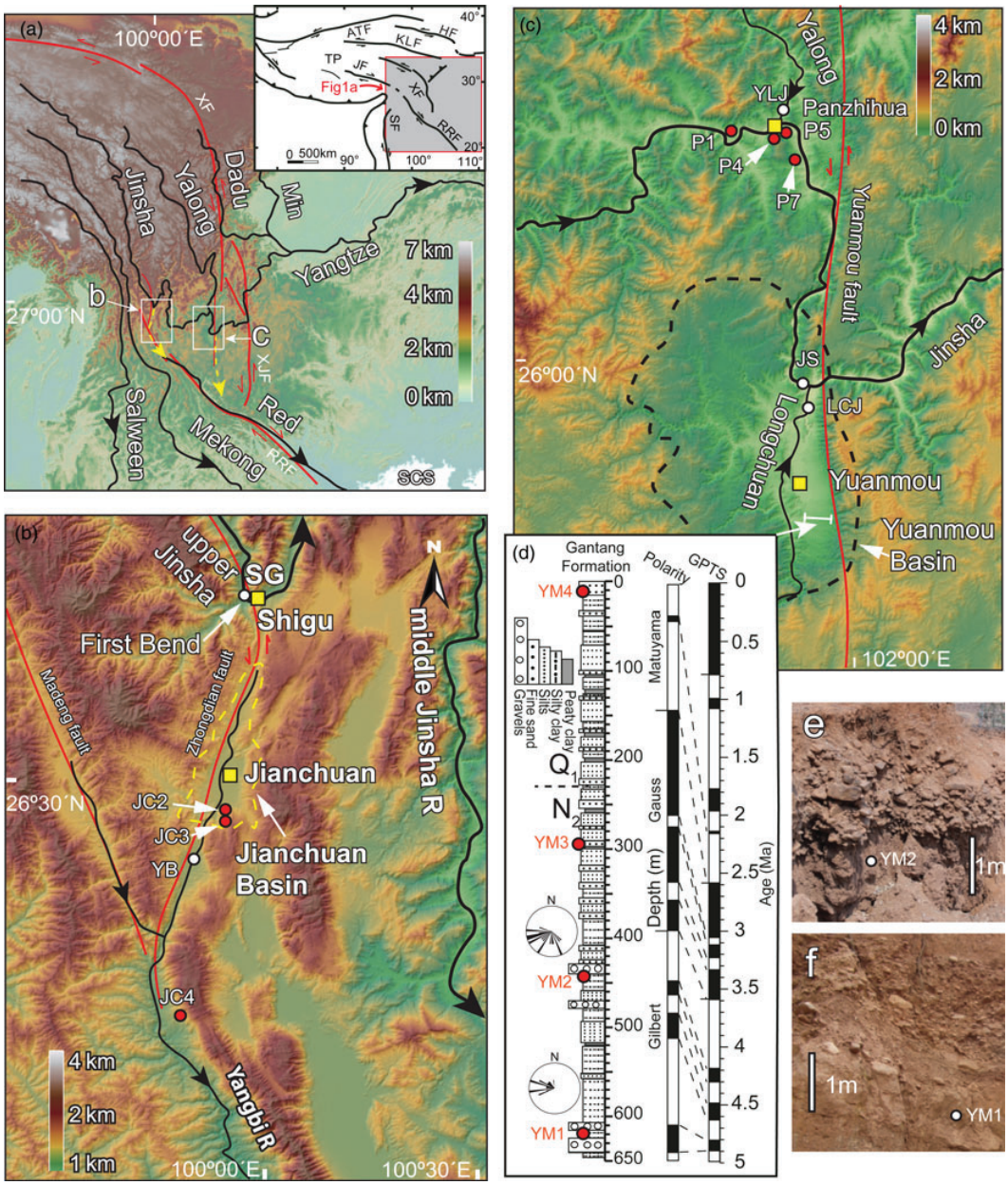

Fig. 1. (**a**) Map showing the study area in SE Tibet. The black lines represent the current rivers. The yellow dashed lines show possible flow paths for the Palaeo-Red River. (**b**) Major rivers and sampling sites in the Jianchuan area. The red dots are locations of samples in this study. The black open circles are sample locations of modern sediments from the Yangbi and Jinsha rivers. (**c**) Major rivers and sampling sites in the Yuanmou–Panzhihua area. (**d**) The stratigraphic position of samples YM1–YM4 (modified from Zhu *et al.* (2008)). (**e**, **f**) Photographs of sampling sites YM1 and YM2. The inset at the top right of (**a**) shows major structures of the Tibetan Plateau. ATF, Altun Tagh fault; HF, Haiyuan fault; JF, Jiali fault; KLF, Kunlun fault; RRF, Red River fault; SCS, South China Sea; SF, Sagaing fault; TP, Tibetan Plateau. XF, Xianshuihe fault; XJF, Xiaojiang fault (modified from Fan *et al.* (2006)). GPTS, geomagnetic polarity timescale.

between the pre-Miocene and Pleistocene formation of the current Yangtze.

In this study, we use total fusion single muscovite and biotite $^{40}Ar/^{39}Ar$ ages and muscovite geochemistry from SE Tibet to document the effect of sediment recycling, and further to reconstruct sediment provenances and the evolution of the upper Yangtze River. Muscovite and biotite have a lower hardness and closure temperatures (350–425°C and 300–350°C, respectively; McDougall and Harrison 1999; Harrison *et al.* 2009) than zircon. Therefore, these minerals break down more easily during sediment reworking and thus are more likely, when found, to record the younger history or latest orogenic cycle. However, muscovite and biotite $^{40}Ar/^{39}Ar$ dating has two disadvantages as a provenance tool: (1) owing to their lower closure temperatures, the age distributions of detrital muscovite and biotite grains could be affected by significant variation in erosion rate of the source area; (2) large spreads in muscovite and biotite do not necessarily reflect a mixture of sources, but could reflect partial resetting by multiple heating events. These potential biases should be kept in mind when interpreting various provenance scenarios (Haines *et al.* 2004).

By application of a combination of the detrital mica $^{40}Ar/^{39}Ar$ dating and multiple muscovite geochemistry methods to 15 Cenozoic fluvial and lacustrine samples collected from SE Tibet,

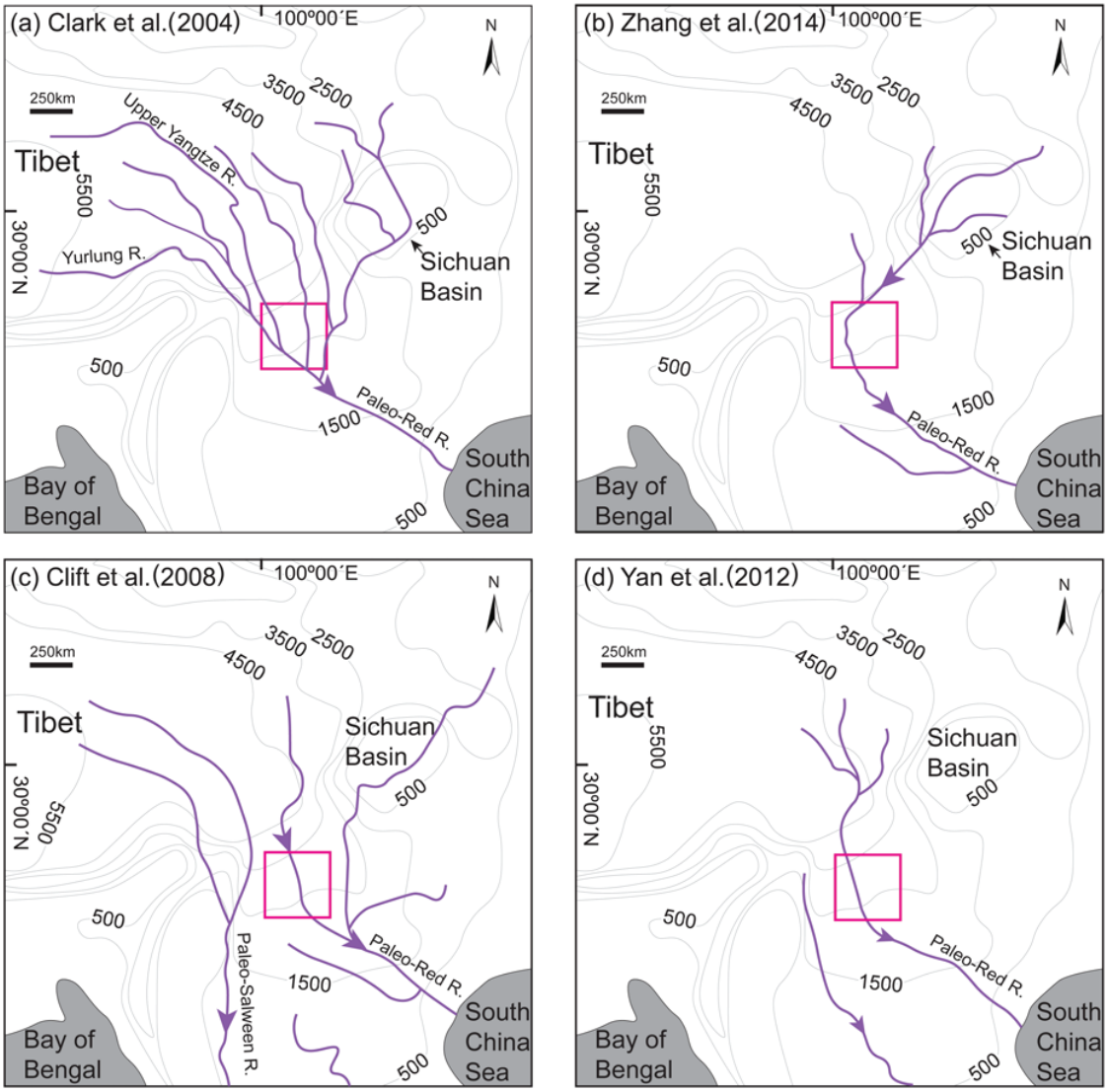

Fig. 2. Summary of possible drainage patterns of the Palaeo-Red River reconstructed by (**a**) Clark *et al.* (2004), (**b**) Zhang *et al.* (2014), (**c**) Clift *et al.* (2008) and (**d**) Yan *et al.* (2012). The purple lines represent rivers and arrows indicate flow direction. The red squares indicate the approximate location of the study area.

we aim to provide more robust constraints on sediment recycling and the evolution history for the Yangtze River drainage system.

Geological setting and samples

Geological setting

The upper Yangtze River drainage system consists of the Jinsha, Yalong and Min rivers and covers most of the Eastern Tibetan Plateau. Samples analysed in this study were collected from the Jianchuan, Panzhihua and Yuanmou areas (Fig. 1). The study area is located along the main stream of the upper Yangtze River and is bounded by two major fault zones, the Xianshuihe–Xiaojiang fault to the NE and the Red River fault to the SW (Fig. 1). Geological and geodetic observations indicate that the area has been undergoing southeastward extrusion and clockwise rotation since Eocene time (England and Molnar 1990; Leloup *et al.* 1995; Tian *et al.* 2014). The activity of these faults may have contributed to the reorganization of the river system in SE Tibet.

The Jianchuan Basin is located *c.* 30 km south of the so-called 'First Bend', an abrupt turn of flow direction from southeastward to northeastward at Shigu Town (Fig. 1b). Cenozoic strata are well exposed in the western part of the Jianchuan Basin, including the Mengyejing Formations (Paleocene), the Baoxiangsi Formation, the Shuanghe Formation and the Jianchuan Formation (upper Eocene), and the Sanying Formation (lower Pliocene) (Gourbet *et al.* 2017). The Sanying Formation unconformably overlies Paleozoic to early Cenozoic sediments (Wang *et al.* 1998). The early Cenozoic sediments are intruded by a series of sub-volcanic syenites and trachytes dated at 40–30 Ma and providing tight age constraints for the Paleocene–late Eocene formations (Wang *et al.* 2001). It is worth noting that previous studies suggested that the fluvial Baoxiangsi Formation could be interpreted as the sedimentary record of the Palaeo-Jinsha River flowing south into the Red River, via the Jianchuan Basin (Clark *et al.* 2004; Yan *et al.* 2012). The Baoxiangsi Formation corresponds to massive quartz sandstones showing cross-bedding with some basal conglomerates. The Baoxiangsi sandstone is of red–grey colour, fine grained and well sorted, lacking dark minerals. The Panzhihua and Yuanmou areas (Fig. 1c) are located in the northern part of the Yunnan terrane. The Panzhihua area is characterized by widespread hundreds of metres thick Quaternary lacustrine sediments (Fig. 3b) that have been dated

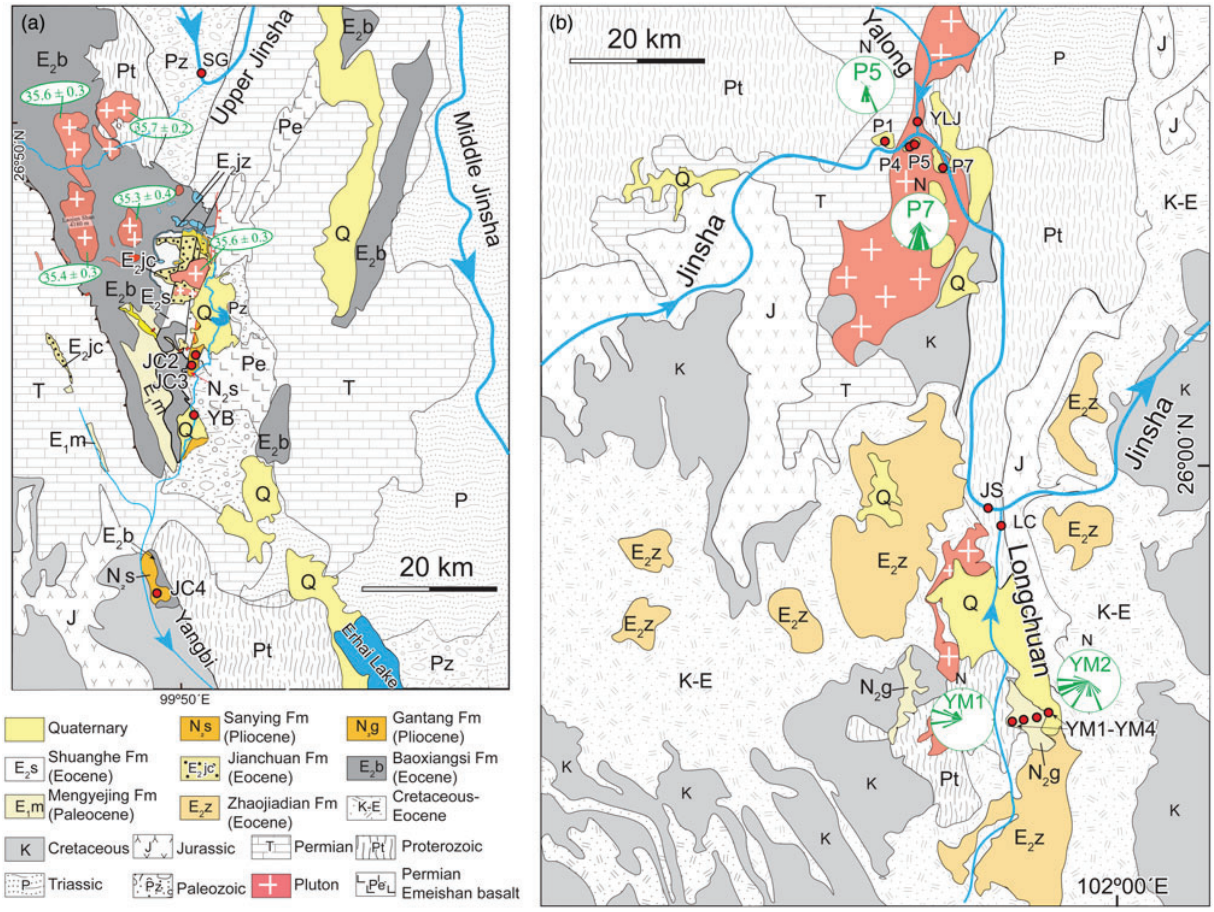

Fig. 3. Geological map of study area. (**a**) Detailed geological map of the Jianchuan area. The ages (numbers in green) of plutons are from Gourbet *et al.* (2017). (**b**) Geological map of the Yuanmou–Panzhihua area with rose diagrams of flow directions.

using ^{26}Al and ^{10}Be cosmogenic dating to 1.34–1.58 Ma by Kong *et al.* (2009). To the south of the Panzhihua, more than 650 m thick late Neogene fluvio-lacustrine sediments (Gantang Formation) are exposed in the Yuanmou Basin (Fig. 1d). The depositional ages of these sediments range from 4.9 to 1.4 Ma based on palaeomagnetic data (Zhu *et al.* 2008). The Palaeo-Yalong River was proposed to flow southward through the Yuanmou Basin (Ting 1933; Zheng 2015).

Sample strategy and description

As proposed above, the Palaeo-Jinsha and Palaeo-Yalong rivers may have flowed south into the Red River, via the Jianchuan and Yuanmou basins, respectively (Fig. 1a). We therefore focused our study on the provenances of Cenozoic sediments preserved in these basins. Our samples cover post-Pliocene sediments in the Jianchuan and Yuanmou basins. For comparison, we also sampled current river sands of the Jinsha, Yalong, Yangbi (a local stream of the Jianchuan Basin) and Longchuan (a local stream of the Yuanmou Basin) rivers. In total, 15 samples were collected from the Jianchuan (five samples), Panzhihua (four samples) and Yuanmou (six samples) areas. Their depositional age constraints are summarized in Table 1. Sample details are introduced below.

In the Jianchuan Basin, three fluvial deposit samples (JC2, JC3 and JC4) were collected (Figs 1b and 3a, and Table 1) from the Pliocene Sanying Formation, which has been dated using cosmogenic nuclides burial dating (Zheng *et al.* 2014). To characterize modern river sand signals, river sand samples were collected and analysed (Fig. 1b and Table 1), including one sample (SG) taken from the Jinsha River near Shigu town and the other (YB) from the modern Yangbi River, which now flows south into the Mekong River.

Near Panzhihua city, where the Yalong flows into the Jinsha River, two sand samples (P1 and P5) were collected from the Pleistocene lacustrine sediments in the Jinsha River valley (Figs 1c and 3b). Two samples (P4 and P7) were collected from fluvial sediments stratigraphically beneath the lacustrine sediments (^{26}Al/^{10}Be burial ages 1.34–1.58 Ma; Kong *et al.* 2009). It is worth noting that samples P1, P4 and P5 are located upstream of the Yalong–Jinsha confluence, whereas sample P7 originates from downstream of the confluence.

Four fluvial sand samples (YM1–YM4) were collected from Pliocene sediment of the Yuanmou Basin (Figs 1b and 3b). The depositional age of these sediments is constrained to early Pliocene–early Pleistocene by previous magnetostratigraphic studies (Zhu *et al.* 2008). Further, two modern river sand samples (JS and LCJ) were sampled from the modern Jinsha main trunk and the Longchuan river (a tributary of the Jinsha River) (Fig. 1b).

Analytical methods

Medium-sized (200–500 μm) muscovite and biotite grains were separated from 15 samples using conventional heavy liquid and magnetic separation techniques. Samples were handpicked under a binocular microscope to remove grains with signs of visible weathering or inclusions. The muscovite fraction was randomly

Table 1. *Summary of sample information*

Location and sample	Description	Latitude (N)	Longitude (E)	Mineral	Depositional age (Ma)		
					Age (Ma)	Dating method	References
Panzhihua							
P1	Lacustrine	26°36'16"	101°32'20"	Ms and Bt	1.36–2.73	$^{26}Al/^{10}Be$ burial age	Kong *et al.* (2009)
P4	Lacustrine	26°34'52"	101°44'02"	Ms and Bt	*c.* 1.34	$^{26}Al/^{10}Be$ burial age	Kong *et al.* (2009)
P5	Fluvial	26°34'53"	101°44'03"	Ms and Bt	1.34–1.89	$^{26}Al/^{10}Be$ burial age	Kong *et al.* (2009)
P7	Fluvial	26°34'01"	101°50'27"	Ms and Bt	>1.58	$^{26}Al/^{10}Be$ burial age	Kong *et al.* (2009)
Yuanmou							
LCJ	Modern sediment	25°57'44"	101°53'01"	Ms and Bt	n.a.	–	n.a.
JS	Modern sediment	25°57'45"	101°53'01"	Ms and Bt	n.a.	–	n.a.
YM4	Fluvial	25°38'56"	101°53'42"	Ms	Early Pleistocene	Palaeomagnetism	Zhu *et al.* (2008)
YM3	Fluvial	25°38'59"	101°53'17"	Ms	Late Pliocene	Palaeomagnetism	Zhu *et al.* (2008)
YM2	Fluvial	25°38'33"	101°51'55"	Ms	Early Pliocene	Palaeomagnetism	Zhu *et al.* (2008)
YM1	Fluvial	25°38'39"	101°50'39"	Ms	Early Pliocene	Palaeomagnetism	Zhu *et al.* (2008)
Jianchuan							
JC2	Fluvial	26°32'22"	99°53'47"	Ms and Bt	Pliocene	$^{26}Al/^{10}Be$ burial age	Zheng *et al.* (2014)
JC3	Fluvial	26°26'51"	99°53'21"	Ms and Bt	Pliocene	$^{26}Al/^{10}Be$ burial age	Zheng *et al.* (2014)
JC4	Fluvial	25°59'01"	99°48'37"	Ms	Pliocene	Plant fossils	Kou *et al.* (2006)
YB	Modern sediment	26°21'30"	99°51'32"	Ms and Bt	n.a.	–	n.a.
SG	Modern sediment	26°52'24"	99°57'43"	Ms and Bt	n.a.	–	n.a.

Modern sediments are sampled using methods as described by Sun *et al.* (2016). Mineral indicates mineral types separated for analysis (Ms, muscovite; Bt, biotite). n.a., not applicable.

split into two aliquots for either chemical analysis or age determination.

Microprobe analysis

The muscovite grains from the first aliquot were embedded in epoxy resin, polished to expose an internal surface and carbon coated for electron microprobe analysis. The major element geochemistry of muscovite grains was determined by a JXA-8530F HyperProbe Electron Probe Microanalyzer at the Electron Microprobe Laboratory, Utrecht University, Netherlands. Wavelength-dispersive spectrometers were used with 20 nA beam current and 15 kV accelerating voltage. The Si, Fe, Mg and Al content of muscovite in metamorphic rocks is variable according to the Tschermak substitution $(Mg^{2+} + Fe^{2+})^{[VI]} + Si^{4+[IV]} = Al^{3+[IV]} + Al^{3+[VI]}$ (Massonne and Szpurka 1997). We therefore use the chemical composition of these elements in muscovite to place constraints on sediment provenance in this study.

$^{40}Ar/^{39}Ar$ dating

The muscovite grains from the second aliquot and biotite were wrapped into 6 mm Al-foil packages and placed into discs with a diameter of 18.8 mm and depth of 3.3 mm for irradiation. An in-house standard, Drachenfels sanidine (DRA; 25.52 ± 0.08 Ma) was used to monitor the neutron flux variation (J). Samples and standards were irradiated for 18 h in the CLICIT Facility in Oregon State University Radiation Center. After irradiation single muscovite grains were loaded into 2 mm diameter holes of a 185-hole copper disc. This disc was pre-baked overnight in a vacuum chamber at 250°C to reduce contaminant air followed by baking in an ultrahigh-vacuum chamber at 120°C connected to a purification line and mass spectrometer. Total fusion analyses of single muscovite grains were performed using a 25W Synrad CO_2 Laser Instrument. The released gas was first purified by a cold trap (−70°C) to trap volatiles and then further cleaned in an ultrahigh-vacuum gas purification line by exposure to SAES NP10 (Fe–V–Zr alloy) getters. The Ar isotopes were measured by a ThermoFisher Helix MC multi-collector noble gas mass spectrometer (Helix) or Hiden HAL 3F Series 1000 Pulse Ion Counting Triple Filter quadrupole mass spectrometer (AGES). Full analytical results are given in the supplementary material (Appendix A (Muscovite) and B (Biotite)) (Figs 4 and 5). The software ArArCALC2.5 (Koppers 2002) was used for data reduction and age calculation.

The number of analysed grains per sample depends on the complexity of detrital age distribution. Samples with simple, unimodal age distributions require only a few dozen grains, whereas those with more complex, multimodal age distributions require more than 100 grains (Vermeesch 2004). For most of the samples, 30–60 grains were analysed, ensuring with 95% certainty that fractions higher than 15% were identified from the underlying population (Vermeesch 2004).

Palaeocurrent data from cobbles

In addition to chemical data and age constraints, palaeocurrents are determined by measuring the orientation of *a*-axes (the trend of the longest axis) of cobbles as identified in the sections. Twenty cobbles per stratigraphic level of samples YM1, YM2, P4 and P7 were measured in the field and plotted in a rose diagram to show the flow direction of the river (Fig. 3b).

Multidimensional scaling

A standard statistical technique called multidimensional scaling (MDS) is used to assess previously reported detrital zircon data and identify similarities and differences between samples from the Jinsha river valley (Vermeesch 2013). The MDS configuration allows a graphical assessment of the salient similarities and differences between samples. The MDS produces a 'map' of points on which 'similar' samples cluster closely together and 'dissimilar' samples plot far apart (for more details, see Vermeesch 2013).

Results

Microprobe analysis

Detailed results of microprobe analyses of 220 muscovite grains from 12 samples are listed in the supplementary material (Appendix C) and shown in Figure 6. Samples JC2, YM1 and MY3 yield insufficient muscovite grains for microprobe analysis.

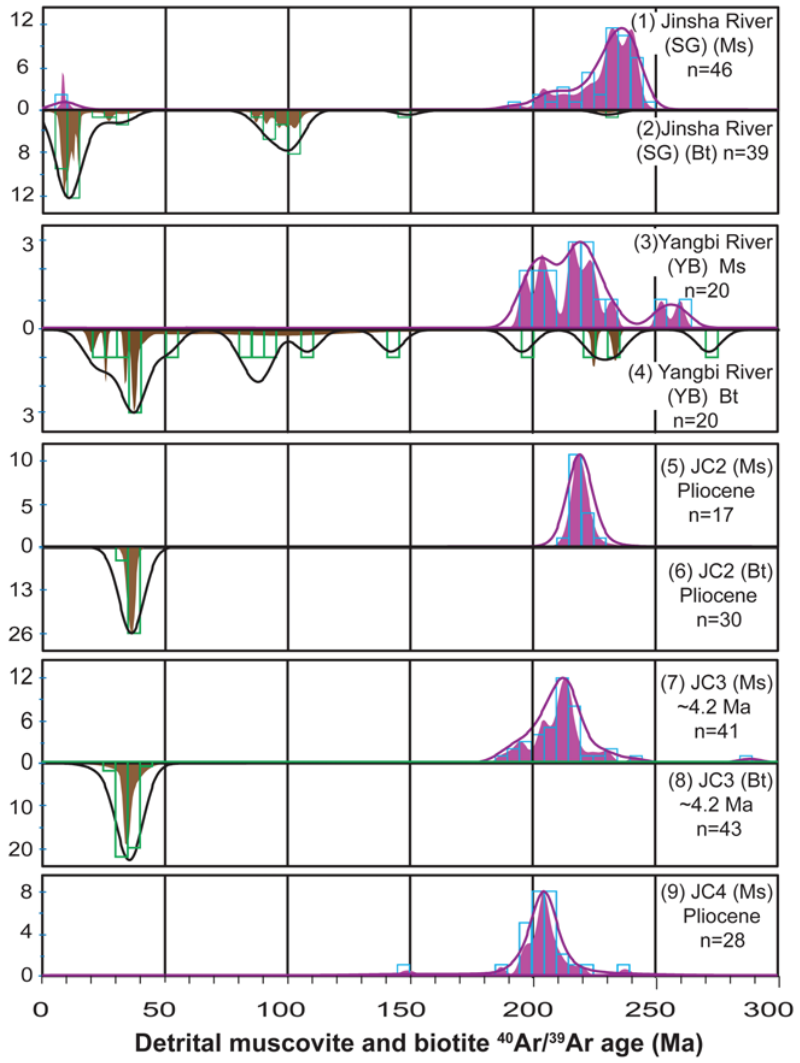

Fig. 4. Muscovite and biotite $^{40}Ar/^{39}Ar$ age distributions of samples from the Jianchuan area. The purple lines and purple shaded areas are respectively kernel density estimations (KDE) and probability density plots (PDP) of muscovites. The black lines and brown shaded areas are respectively KDEs and PDPs of biotites.

Jianchuan area

Muscovite grains from sample JC3 display bimodal chemical distributions and overlap partly with the upper Jinsha River field (Fig. 6a). Phengite grains (four out of eight grains) were observed in sample JC3 (Fig. 6a). The data points of sample JC4 plot in the geochemical fields of the Yangbi and upper Jinsha rivers (Fig. 6a).

Yuanmou area

The muscovite geochemistry of fluvial sample YM4 (Early Pleistocene) is generally identical to that found for the Longchuan River (Fig. 6b). Some of the muscovites from fluvial sample YM2 (early Pliocene) overlap with the signals for the lower Jinsha (JS) and Longchuan rivers.

Panzhihua area

Most data points of early Pleistocene lacustrine and fluvial samples P1, P4 and P5 plot in the fields for the upper Jinsha River (sample SG: watershed above the First Bend) (Fig. 6c). The Yalong River also can be a potential source for some muscovite grains in these samples. The chemical compositions of muscovites from early Pleistocene fluvial sample P7 are similar to those of the Yalong River (Fig. 6c).

$^{40}Ar/^{39}Ar$ dating of muscovite

In total, 562 muscovite $^{40}Ar/^{39}Ar$ ages from 15 samples were dated for this study.

Jianchuan area

Muscovite grains from the Pliocene fluvial samples JC2, JC3 and JC4 yielded similar age distributions (Fig. 4). Most of the muscovites from these samples are distributed between 180 and 240 Ma, with major peaks at 220 Ma (JC2), 213 Ma (JC3) and 205 Ma (JC4). Modern sand sample YB from the Yangbi River is similar to samples JC2, JC3 and JC4 and is dominated by an age cluster at 195–235 Ma (Fig. 4).

Yuanmou area

In the Yuanmou area all muscovite grains from the samples YM4 (Early Pleistocene) and YM1 (early Pliocene) are distributed between 580 and 800 Ma with major peaks at 760 Ma (YM1) and 740 Ma (YM4), respectively (Fig. 5). This age population overlaps well with the 660–800 Ma population of the Longchuan River (Fig. 5). The age distributions of samples YM2 (early Pliocene) and YM3 (late Pliocene) are more complex and overlap with those of the lower Jinsha (JS) and Yalong rivers (Fig. 5).

Panzhihua area

In the Panzhihua area Pleistocene samples P1 and P5 have similar age distributions, with a large proportion of the muscovite ages being between 10–30 and 200–240 Ma, suggesting that they have similar sources (Fig. 5). Approximately 93% of the muscovites in sample P4 are in an age range of 220–240 Ma, similar to the upper

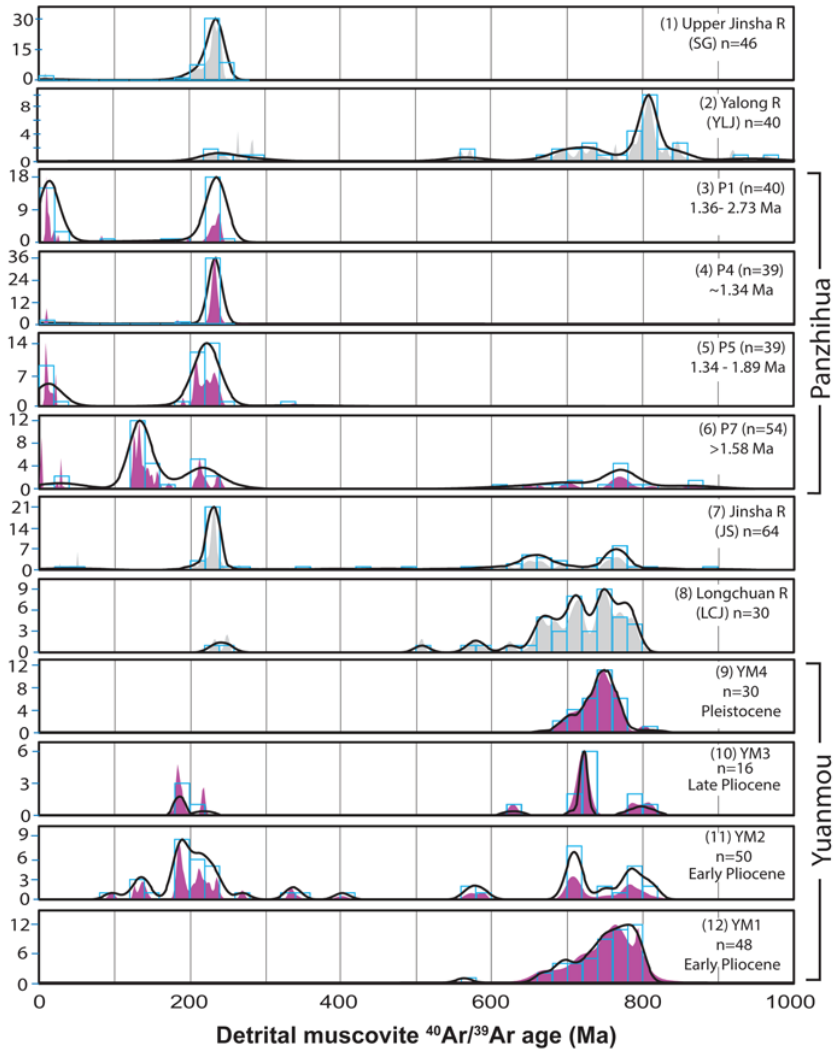

Fig. 5. Muscovite $^{40}Ar/^{39}Ar$ age distributions of samples from the Panzhihua and Yuanmou areas. The black lines and shaded areas are respectively KDEs and PDPs of muscovites. Muscovite ages of the Yalong River are from Sun *et al.* (2016). The difference in age scale (0–1000 Ma) in comparison with Figure 3 (0–300 Ma) should be noted.

Jinsha River (SG). Sample P7 is dominated by an age population of 120–160 Ma, accounting for *c*. 52% of the total dated grains. Another 45% of muscovite grains in sample P7 are distributed between 200–240 and 600–900 Ma, overlapping with the Yalong River.

$^{40}Ar/^{39}Ar$ dating of biotite

In total, 123 biotites from the Jianchuan Basin were dated in this study (Fig. 4). Sample JC4 yielded insufficient biotite grains for $^{40}Ar/^{39}Ar$ dating. Thirty-nine detrital biotite grains from the upper Jinsha River (SG) showed a dominant population of 5–25 Ma (*c*. 62%) and a minor population of 80–92 Ma (*c*. 27%), which is significantly different from samples YB, JC2 and JC3 (Fig. 4). All detrital biotite ages of samples JC2 and JC3 are distributed between 20 and 40 Ma, similar to the signal found for the Yangbi River (YB) (Fig. 4).

Discussion

Sediment provenance and reworking

As introduced above, previous studies suggested that the upper Jinsha River used to flow southward through the Jianchuan Basin into the Red River, and then lost its connection with the upper reaches to flow eastward via the Yuanmou basin into the current Yangtze (Brookfield 1998; Clark *et al.* 2004). Therefore, changes in sediment provenances are expected to have occurred in the Jianchuan and Yuanmou basins, which will be discussed below.

Sediment provenance in the Jianchuan area

The biotite age distributions of Pliocene sediments (JC2 and JC3) overlap with those of the Yangbi River, but are different from those of the upper Jinsha River (SG), indicating that these biotite grains were not derived from the upper Jinsha River. Because the Eocene rocks in the Jianchuan Basin are the source of the Yangbi River signal, it is not surprising that biotite age distributions of these Pliocene samples are similar to that of the Yangbi River. The biotite $^{40}Ar/^{39}Ar$ and zircon U–Pb ages (*c*. 35 Ma) of trachytes and syenites (Gourbet *et al.* 2017) in the Jianchuan Basin (Fig. 3a) are in agreement with the major biotite age peak of *c*. 35 Ma in Pliocene sediments (Fig. 4). This demonstrates that these widespread trachytes and syenites in the Jianchuan Basin probably are the source of the biotite grains in the Pliocene sediment in the Jianchuan Basin and not the source of the muscovites, as these are not present in the trachyte and syenite source rocks (Fig. 7).

In contrast, the muscovite age distributions of the Pliocene sediment in the Jianchuan Basin show a different picture. The overlapping age populations of the Pliocene samples suggest that most of them were derived from a single source area (Fig. 4). The major muscovite age populations of these samples partly overlap

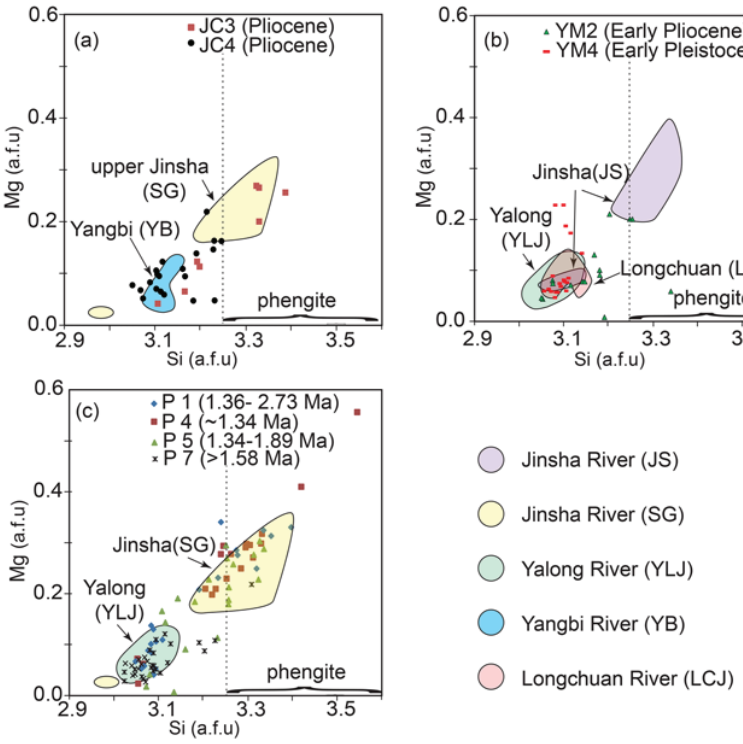

Fig. 6. (**a**–**c**) Muscovite geochemistry of samples from the Jianchuan Basin, Yuanmou Basin and Panzhihua area. Muscovite Si and Mg concentration of Jinsha River near the Yuanmou Basin (JS; purple polygon), the first bend (SG; yellow polygon), the Yalong River (YLJ; light cyan polygon), Yangbi River (YB; blue polygon) and Longchuan River (LCJ; pink polygon) are muscovite data for modern sediment.

with those of the upper Jinsha (sample SG) and Yangbi (YB) rivers (Fig. 4), suggesting that the muscovites are likely to be derived from the palaeo-upper Jinsha or Yangbi river basin. The presence of four phengite grains (four of eight) (Si > 3.25) in JC3 implies that some muscovite grains are likely to have originated from high-pressure rocks as currently exposed in the Qiangtang region in the upper Jinsha River (Kapp *et al.* 2003). The $^{40}Ar/^{39}Ar$ ages of phengites (210–230 Ma) in the Qaingtang region are also consistent with the dominant muscovite age population of the Pliocene sediment (200–230 Ma). Therefore, we suggest that some of the muscovite grains in the Pliocene sediment were derived from the upper Jinsha River (Fig. 7).

Sediment reworking in the Jianchuan area

Significantly, muscovite and biotite grains from the same samples (JC2–JC4) indicate different sources. To explain this, we propose that these Pliocene sediments have experienced sediment reworking

Sample	Age	Direct supplier	Indirect supplier	Locality of source area
JC2	Pliocene	Sedimentary rocks and trachytes in the Jianchuan Basin	Paleo-upper Jinsha River	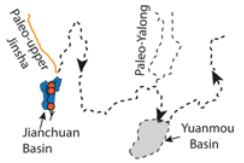
JC3				
JC4				
YM4	Pliocene - Pleistocene	Cretaceous - Paleogene sediments in the Yuanmou Basin	Paleo-Jinsha River (including paleo-Yalong River)	
YM3				
YM2				
YM1				
P1	Early Pleistocene	Upper Jinsha and unsampled small tributaries	———	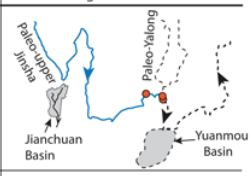
P4				
P5				
P7	Early Pleistocene	Yalong and upper Jinsha rivers	———	

Fig. 7. Summary of sediment provenance interpretations for Pliocene sediments in Jianchuan Basin (upper panel), Early Pleistocene sediments near Panzhihua (two lower panels) and Pliocene–Pleistocene sediments in the Yuanmou basin (middle panel). Red circles indicate sample locations. The continuous blue lines or blue areas indicate the direct sediment suppliers to ancient samples in this study. The orange lines indicate indirect sediment supplier (recycled sediment) to ancient samples. The dashed lines represent non-suppliers.

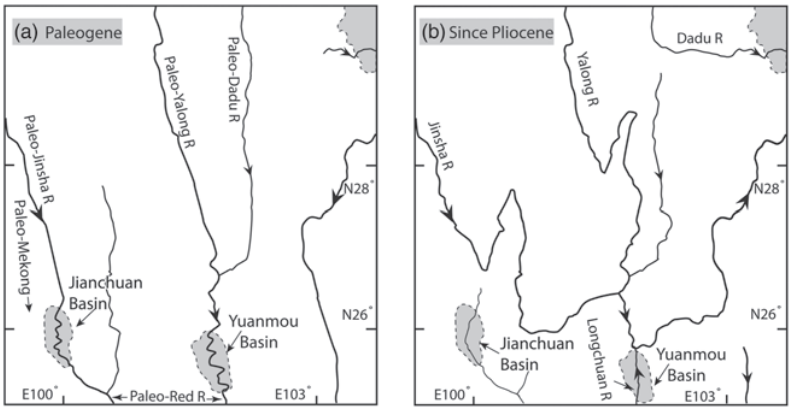

Fig. 8. Reconstruction of the Palaeo-Yangtze River. (**a**) In the pre-Pliocene, prior to capture, the Palaeo-Jinsha and Palaeo-Yalong rivers flowed into the Palaeo-Red River. (**b**) After capture in the Pliocene, the Palaeo-Jinsha and Palaeo-Yalong rivers were redirected to flow east to form the modern Yangtze drainage system. Black lines, rivers; grey areas, basins. Black arrows indicate flow directions.

in the Jianchuan Basin. The age consistency between detrital biotite of the Pliocene sediments and the local trachytes and syenites suggests that the sediments were probably locally derived from the widespread trachytes and syenites exposed in the Jianchuan Basin, thus indicating a local derivation of the Pliocene sediment. The muscovite in the Pliocene sediments was probably sourced from the local Eocene Baoxiangsi Formation, which was derived from the Palaeo-Jinsha River, as indicated by previous zircon U–Pb data (Yan *et al.* 2012). As the Eocene trachytes and syenites are poor in muscovite (Liu *et al.* 2017), no Eocene ages are observed in our muscovite detrital results.

In such a reworking scenario we need an explanation for the absence of Jinsha-derived biotites in the Pliocene sediments (Fig. 4). We think the absence of Jinsha biotites is caused by the following reasons. First, biotite is less resistant to physical and chemical attack compared with muscovite and thus has a shorter lifetime (Kowalewski and Rimstidt 2003). The Paleogene Baoxiangsi Formation, which contains mostly quartz sandstone, is very poor in biotite, probably because of Eocene weathering and long transport into the Jianchuan Basin. Second, during Pliocene reworking, abundant biotite from Eocene trachytes and syenites further diluted the biotite from the Paleogene Baoxiangsi Formation, explaining the absence of the Jinsha biotite in our Jianchuan Pliocene samples (JC2–JC4). Our data suggest that biotite is more likely to indicate direct sediment source whereas muscovite could survive two and even more cycles of deposition and erosion.

Provenance of sediment in the Yuanmou area (Pliocene–early Pleistocene)

Early Pliocene (YM1) and early Pleistocene sediments (YM4) have similar age distributions, suggesting that these samples have similar sources. Their age populations overlap with those of the Longchuan River (LCJ), suggesting a derivation of sediment from a similar river catchment area that is currently drained by this river (Fig. 5). This is also supported by the overlap in muscovite geochemistry between Pleistocene sediments (YM4) and Longchuan River (LCJ) (Fig. 6b).

The muscovite age distributions of the Pliocene sediment (YM2 and YM3) roughly overlap with those of the Yalong (YLJ) and Jinsha (JS) rivers (Fig. 5). A direct interpretation is that the muscovites in these samples were derived from the Palaeo-Jinsha River (including the Palaeo-Yalong River). However, we propose a different scenario in that the Pliocene sediments in the Yuanmou Basin are likely to be recycled from the late Cretaceous–Eocene sediments in and near the Yuanmou Basin instead of being directly derived from the drainage basin of the Palaeo-Jinsha River (including the Palaeo-Yalong River) for the following three reasons. First, the west-southwest-ward palaeocurrent measurements from cobbles above the early Pliocene samples (YM1 and YM2) (Fig. 3b) show that these sediments might originate from upper Cretaceous–Paleogene sandstones located in the east of the Yuanmou Basin (Fig. 3b). Second, the early Pliocene sediments are poorly sorted with sub-angular cobbles and sandstones (Fig. 1d), implying a relatively local derivation. Third, zircon, apatite and rutile U–Pb data from the nearby late Cretaceous–Eocene sediments (Deng *et al.* 2018) suggest that the late Cretaceous–Eocene sediments might be derived from the Palaeo-Jinsha River basin. These late Cretaceous–Eocene strata were probably eroded and recycled to source the Pliocene sediments, explaining the similarities in muscovite age and geochemistry data between Pliocene samples (YM2 and YM3) and the Jinsha River (JS) (Fig. 7).

Provenance of sediments in the Panzhihua area

The major age peaks in the populations of muscovite grains from lower Pleistocene sediment (P1, P4 and P5) overlap with those of the upper Jinsha River (SG) (Fig. 5), meaning that some of the sediments in these samples were derived from the upper Jinsha River. This interpretation is also supported by muscovite geochemistry and palaeocurrent data (Figs 3b and 6c) and implies an early Pleistocene gateway between Shigu and Panzhihua. We therefore argue that the upper Jinsha River is the most important sediment contributor to lower Pleistocene sediments located upstream of the Yalong–Jinsha confluence (P1, P4 and P5) (Fig. 7). Muscovite age distributions of lower Pleistocene sample (P7) from downstream of the Yalong–Jinsha confluence overlap with the Yalong (YLJ) and Jinsha rivers (JS), suggesting that Pleistocene sediment at this site is likely to be a mixture of sediments from these rivers. This is in agreement with the rose diagram, which indicates that the palaeocurrent direction at this site is towards the south (Fig. 3b).

Implications for the development of the Jinsha River

Capture event at the First Bend

The spatio-temporal variation in sediment provenance is largely controlled by reorganization of the drainage patterns caused by uplift and/or variation in erosion rate. Detrital zircon U–Pb data suggest that the upper Eocene Baoxiangsi Formation originated from the Palaeo-Jinsha River (Yan *et al.* 2012). The biotites in the Pliocene sediments were not derived from the upper Jinsha River but from rocks in the Jianchuan Basin and demonstrate that the Jianchuan Basin lost its connection with the upper Jinsha River at least before the Pliocene (Fig. 8). Our results are consistent with previous studies (McPhillips *et al.* 2016; Shen *et al.* 2016). Burial ages of samples collected from caves on the walls of the Jinsha

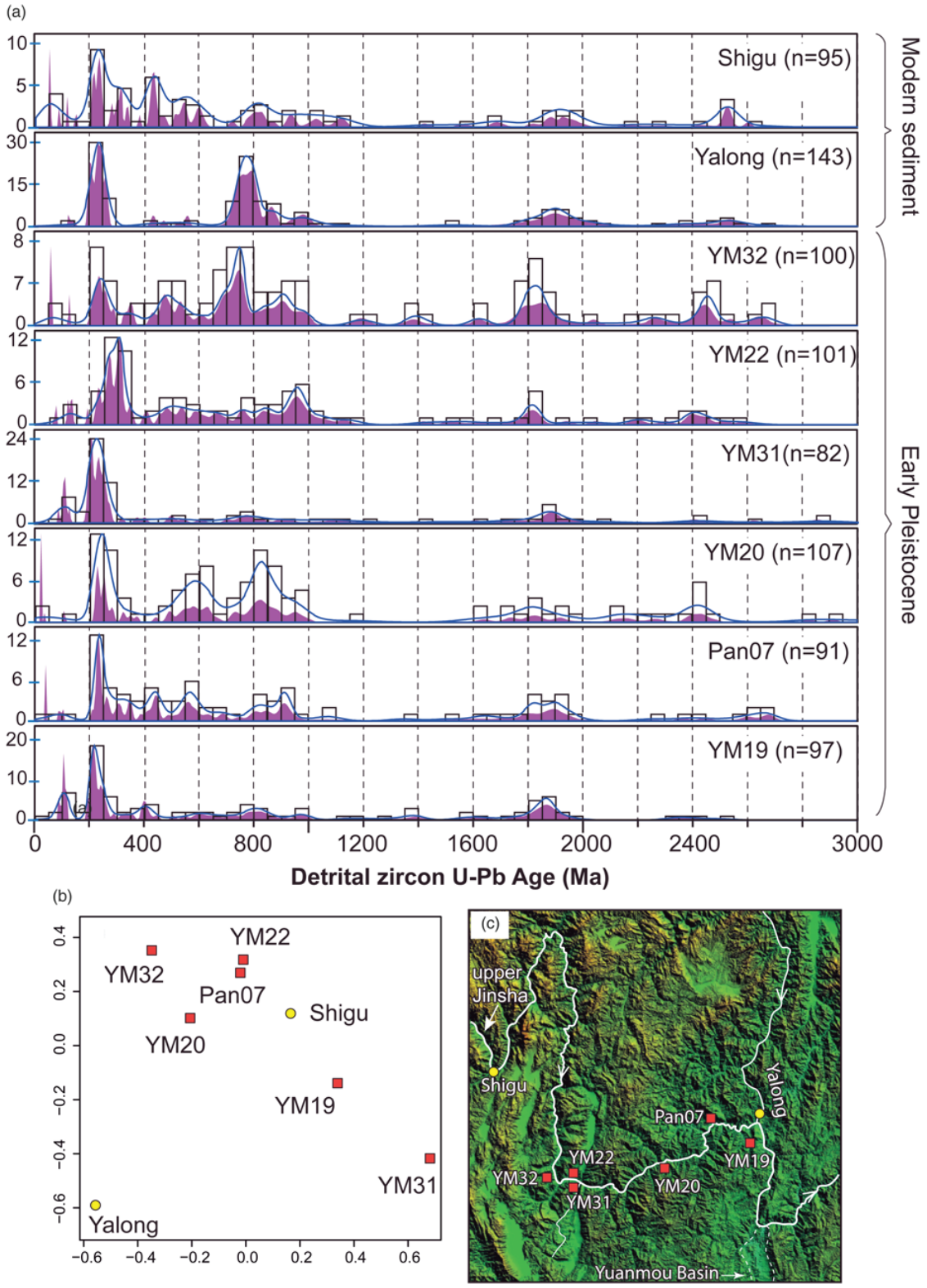

Fig. 9. Reassessment of the detrital zircon data from Kong *et al.* (2009). (**a**) Detrital zircon U–Pb age distributions of fluvial or lacustrine samples from the Jinsha River valley. Sample sites are shown in (**c**). (**b**) Multidimensional scaling (MDS) plot of zircon ages. 'Similar' samples cluster closely together in the MDS. It should be noted that samples from the Jinsha valley plot far away from the Yalong samples, but close to that of the upper Jinsha River (Shigu sample). The red squares and yellow dots represent samples from the Jinsha River valley and modern sediments from Jinsha and Yalong rivers, respectively. Detailed localities are shown in (**c**).

River valley at the First Bend suggest that the Jinsha River channel had incised below the wind gap near the First Bend before 9 Ma (McPhillips *et al.* 2016). Additionally, apatite (U–Th–Sm)/He data from a vertical profile near the First Bend indicate an Oligocene–Early Miocene phase of river incision after the capture event (Shen *et al.* 2016).

Our pre-Pliocene model is inconsistent with the Pleistocene capture and formation of the First Bend model as preferred by other studies (Kong *et al.* 2009, 2012; Zheng *et al.* 2014). The Pleistocene model was built based on detrital zircon U–Pb data from late Cenozoic sediment in and near the Jianchuan Basin. This disagreement could be caused by sediment reworking, as shown by our detrital biotite and muscovite data discussed above. Detrital zircons in late Cenozoic sediments are possibly locally derived from the Eocene Baoxiangsi Formation and probably originate from the Palaeo-Jinsha River.

Capture event in the Yuanmou area

To the east of the Jianchuan Basin, Pliocene sediments in the Yuanmou Basin were derived from Late Cretaceous–Eocene strata in this basin. This scenario is consistent with the lithostratigraphy and sedimentology in the Yuanmou Basin, which suggest that the Pliocene sediments were deposited in a fluvial–lacustrine environment (Urabe *et al.* 2001; Zhu *et al.* 2008), which precludes routing of a large river such as the modern Jinsha River through an intermountain basin like the Yuanmou Basin during the Pliocene (Fig. 8). We suggest that the Palaeo-Jinsha and Red rivers have not been connected since the Pliocene. However, to fully confirm this interpretation, more muscovite age and geochemistry data for the Late Cretaceous–Eocene sediments in the Yuanmou Basin are required.

Formation of river course from Shigu to Panzhihua

Our new data from the Jianchuan and Yuanmou basins suggest that both the upper Jinsha and Yalong rivers did not flow southward into these two basins at least since the Pliocene. Here we discuss the timing of the connection between the upper Jinsha and Yalong rivers. Our muscovite data indicate that the upper Jinsha River is an important sediment contributor to early Pleistocene sediments in the Jinsha River valley in the Panzhihua area. This suggests that the river course from Shigu to Panzhihua had already formed before the early Pleistocene. Derivation of the Pleistocene sediments (P7) from the Yalong River implies that the Yalong River flowed southward into the Jinsha River before the early Pleistocene. In contrast, based on detrital zircon U–Pb ages from the fluvial and lacustrine sediments in the Jinsha River valley near Panzhihua, Kong *et al.* (2009) suggested that the river course from Shigu to Panzhihua formed in the early Pleistocene. However, the differences between the detrital zircon age distributions of samples from the Jinsha River valley are subtle (Fig. 9a); it is difficult to identify their differences or similarities based on visual inspection. The multidimensional scaling (MDS) configuration of detrital zircon data allows a graphical assessment of the salient similarities between samples. The multidimensional scaling map of U–Pb data for samples from the Pleistocene sediments in the Jinsha River valley is in general not similar to that for samples from the Yalong River but is more similar to that of the upper Jinsha River (Fig. 9b), which implies that sediments from the upper Jinsha have been transported to the Panzhihua area in the Pleistocene. This suggests that the river course from Shigu to Panzhihua must have formed before the early Pleistocene, which is consistent with our observation.

Conclusion

A combination of muscovite and biotite ages and muscovite geochemistry provides new constraints on late Cenozoic sediment provenance in SE Tibet and the evolution of the Jinsha and Yalong rivers. Our new data suggest that late Cenozoic sediments in SE Tibet have probably experienced multiple cycles of reworking: sediments in the Jianchuan and Yuanmou basins probably originate from the sedimentary rocks in and near these basins, which were derived from the Palaeo-Jinsha River. This is an important factor in the current debate on either Pleistocene or pre-Miocene formation of the Yangtze River. The constraints on sediment provenance imply that the originally south-flowing Palaeo-Jinsha and Yalong rivers were captured to flow eastwards at least before the Pliocene. The combination of data from the Jianchuan and Yuanmou basins rules out previous models suggesting Pleistocene formation of the Yangtze River.

Acknowledgements B. Uunk is acknowledged for the early review of this paper. We are grateful to M. Brookfield and two anonymous reviewers for helpful suggestions. We also thank Editor P. Clift for editorial handing and constructive comments.

Funding This study was financially supported by the National Natural Science Foundation of China (41671011, 41672355, 41772211 and 41801003), the Guangdong Province Introduced Innovative R&D Team (2016ZT06N331) and the Fundamental Research Funds for the Central Universities (19lgjc03 and 19lgpy72). K.K. is supported by NWO-ALW grant 864.12.005. This work was supported by the argon geochronology laboratory of the Vrije Universiteit Amsterdam.

Author contributions **XS:** conceptualization (lead), data curation (lead), methodology (lead), writing – original draft (lead), writing – review & editing (lead); **KK:** supervision (equal), writing – review & editing (lead); **CL:** funding acquisition (lead); **YT:** writing – review & editing (equal); **LG:** investigation (equal); **ZZ:** writing – review & editing (equal); **RG:** data curation (equal); **VB:** data curation (equal); **JW:** funding acquisition (lead), methodology (lead), writing – original draft (equal), writing – review & editing (lead)

Scientific editing by Peter Clift

References

Barbour, G.B. 1936. Physiographic history of the Changjiang. *Geographical Journal*, **87**, 285–312, https://doi.org/10.2307/1786198

Brookfield, M.E. 1998. The evolution of the great river systems of southern Asia during the Cenozoic India–Asia collision: rivers draining southwards. *Geomorphology*, **22**, 285–312, https://doi.org/10.1016/S0169-555X(97)00082-2

Chen, Y., Yan, M.D. *et al.* 2017. Detrital zircon U–Pb geochronological and sedimentological study of the Simao Basin, Yunnan: Implications for the Early Cenozoic evolution of the Red River. *Earth and Planetary Science Letters*, **476**, 22–33, https://doi.org/10.1016/j.epsl.2017.07.025

Clark, M.K., Schoenbohm, L.M. *et al.* 2004. Surface uplift, tectonics, and erosion of eastern Tibet from large-scale drainage patterns. *Tectonics*, **23**, TC1006, https://doi.org/10.1029/2002TC001402

Clift, P.D., Blusztajn, J. and Duc, N.A. 2006. Large-scale drainage capture and surface uplift in eastern Tibet–SW China before 24 Ma inferred from sediments of the Hanoi Basin, Vietnam. *Geophysical Research Letters*, **33**, L19403, https://doi.org/10.1029/2006GL027772

Clift, P.D., Van Long, H. *et al.* 2008. Evolving east Asian river systems reconstructed by trace element and Pb and Nd isotope variations in modern and ancient Red River–Song Hong sediments. *Geochemistry, Geophysics, Geosystems*, **9**, Q04039,https://doi.org/10.1029/2007GC001867

Deng, B., Chew, D., Jiang, L., Mark, C., Cogné, N., Wang, Z.J. and Liu, S.G. 2018. Heavy mineral analysis and detrital U–Pb ages of the intracontinental Paleo-Yangzte basin: Implications for a transcontinental source-to-sink system during Late Cretaceous time. *Geological Society of America Bulletin*, **130**, 2087–2109, https://doi.org/10.1130/B32037.1

England, P. and Molnar, P. 1990. Right-lateral shear and rotation as the explanation for strike-slip faulting in eastern Tibet. *Nature*, **344**, 140, https://doi.org/10.1038/344140a0

Fan, C., Wang, G., Wang, S.F. and Wang, E.C. 2006. Structural interpretation of extensional deformation along the Dali Fault System, southeastern margin of the Tibetan Plateau. *International Geology Review*, **48**, 287–310, https://doi.org/10.2747/0020-6814.48.4.287

Gourbet, L., Leloup, P.H. *et al.* 2017. Reappraisal of the Jianchuan Cenozoic basin stratigraphy and its implications on the SE Tibetan plateau evolution. *Tectonophysics*, **700–701**, 162–179, https://doi.org/10.1016/j.tecto.2017.02.007

Haines, P.W., Turner, S.P., Kelley, S.P., Wartho, J.A. and Sherlock, S.C. 2004. $^{40}Ar/^{39}Ar$ dating of detrital muscovite in provenance investigations: a case study from the Adelaide Rift Complex, South Australia. *Earth and Planetary Science Letters*, **227**, 297–311, https://doi.org/10.1016/j.epsl.2004.08.020

Hanchar, J.M. 2013. *Zircon*. Springer, Berlin.

Harrison, T.M., Célérier, J., Aikman, A.B., Hermann, J. and Heizler, M.T. 2009. Diffusion of ^{40}Ar in muscovite. *Geochimica et Cosmochimica Acta*, **73**, 1039–1051, https://doi.org/10.1016/j.gca.2008.09.038

Hoang, L.V., Wu, F.-Y., Clift, P.D., Wysocka, A. and Swierczewska, A. 2009. Evaluating the evolution of the Red River system based on *in situ* U–Pb dating and Hf isotope analysis of zircons. *Geochemistry, Geophysics, Geosystems*, **10**, Q11008, https://doi.org/10.1029/2009GC002819

Kapp, P., Yin, A., Manning, C.E., Harrison, T.M., Taylor, M.H. and Ding, L. 2003. Tectonic evolution of the early Mesozoic blueschist-bearing Qiangtang metamorphic belt, central Tibet. *Tectonics*, **22**, 1043, https://doi.org/10.1029/2002TC001383

Kong, P., Granger, D.E., Wu, F.Y., Caffee, M.W., Wang, Y.J., Zhao, X.T. and Zheng, Y. 2009. Cosmogenic nuclide burial ages and provenance of the Xigeda paleo-lake: Implications for evolution of the Middle Yangtze River. *Earth and Planetary Science Letters*, **278**, 131–141, https://doi.org/10.1016/j.epsl.2008.12.003

Kong, P., Zheng, Y. and Caffee, M.W. 2012. Provenance and time constraints on the formation of the first bend of the Yangtze River. *Geochemistry, Geophysics, Geosystems*, **13**, Q06017, https://doi.org/10.1029/2012GC004140

Koppers, A.A.P. 2002. ArArCALC-software for $^{40}Ar/^{39}Ar$ age calculations. *Computers & Geosciences*, **28**, 605–619, https://doi.org/10.1016/S0098-3004(01)00095-4

Kou, X.Y., Ferguson, D.K., Xu, J.X., Wang, Y.F. and Li, C.S. 2006. The reconstruction of paleovegetation and paleoclimate in the Late Pliocene of West Yunnan, China. *Climatic Change*, **77**, 431–448, https://doi.org/10.1007/s10584-005-9039-5

Kowalewski, M. and Rimstidt, J.D. 2003. Average lifetime and age spectra of detrital grains: toward a unifying theory of sedimentary particles. *Journal of Geology*, **111**, 427–439, https://doi.org/10.1086/375284

Lee, J.K.W., Williams, I.S. and Ellis, D.J. 1997. Pb, U and Th diffusion in natural zircon. *Nature*, **390**, 159–162, https://doi.org/10.1038/36554

Leloup, P.H., Lacassin, R. *et al.* 1995. The Ailao Shan–Red River shear zone (Yunnan, China), Tertiary transform boundary of Indochina. *Tectonophysics*, **251**, 3–84, https://doi.org/10.1016/0040-1951(95)00070-4

Liu, Z., Liao, S.Y. *et al.* 2017. Petrogenesis of late Eocene high Ba–Sr potassic rocks from western Yangtze Block, SE Tibet: A magmatic response to the Indo-Asian collision. *Journal of Asian Earth Sciences*, **135**, 95–109, https://doi.org/10.1016/j.jseaes.2016.12.030

Massonne, H.-J. and Szpurka, Z. 1997. Thermodynamic properties of white micas on the basis of high-pressure experiments in the systems K_2O–MgO–Al_2O_3–SiO_2–H_2O and K_2O–FeO–Al_2O_3–SiO_2–H_2O. *Lithos*, **41**, 229–250, https://doi.org/10.1016/S0024-4937(97)82014-2

McDougall, I. and Harrison, T.M. 1999. *Geochronology and Thermochronology by the $^{40}Ar/^{39}Ar$ Method*. Oxford University Press, Oxford.

McPhillips, D., Hoke, G.D., Jing, L.-Z., Bierman, P.R., Rood, D.H. and Niedermann, S. 2016. Dating the incision of the Yangtze River gorge at the First Bend using three-nuclide burial ages. *Geophysical Research Letters*, **43**, 101–110, https://doi.org/10.1002/2015GL066780

Shen, X.M., Tian, Y.T., Li, D.W., Qin, S.W., Vermeesch, P. and Schwanethal, J. 2016. Oligocene–Early Miocene river incision near the first bend of the Yangze River: Insights from apatite (U–Th–Sm)/He thermochronology. *Tectonophysics*, **687**, 223–231, https://doi.org/10.1016/j.tecto.2016.08.006

Sun, X.L., Li, C.A., Kuiper, K.F., Zhang, Z.J., Gao, J.H. and Wijbrans, J.R. 2016. Human impact on erosion patterns and sediment transport in the Yangtze River. *Global and Planetary Change*, **143**, 88–99, https://doi.org/10.1016/j.gloplacha.2016.06.004

Tian, Y.T., Kohn, B.P., Gleadow, A.J.W. and Hu, S.B. 2014. A thermochronological perspective on the morphotectonic evolution of the southeastern Tibetan Plateau. *Journal of Geophysical Research: Solid Earth*, **119**, 676–698, https://doi.org/10.1002/2013JB010429

Ting, V. 1933. The south bank of Jingshajiang–Wuding and Yuanmou. *Independence Review*, p. 48.

Urabe, A., Nakaya, H., Muto, T., Katoh, S., Hyodo, M. and Xue, S.R. 2001. Lithostratigraphy and depositional history of the Late Cenozoic hominid-bearing successions in the Yuanmou Basin, southwest China. *Quaternary Science Reviews*, **20**, 1671–1681, https://doi.org/10.1016/S0277-3791(01)00023-3

Vermeesch, P. 2004. How many grains are needed for a provenance study? *Earth and Planetary Science Letters*, **224**, 441–451, https://doi.org/10.1016/j.epsl.2004.05.037

Vermeesch, P. 2013. Multi-sample comparison of detrital age distributions. *Chemical Geology*, **341**, 140–146, https://doi.org/10.1016/j.chemgeo.2013.01.010

Wang, E., Burchfiel, B.C., Royden, L.H., Chen, L.Z., Chen, J.S., Li, W.X. and Chen, Z.L. 1998. Late Cenozoic Xianshuihe–Xiaojiang, Red River, and Dali Fault Systems of Southwestern Sichuan and Central Yunnan, China. Geological Society of America, Special Papers, **327**, 1–108.

Wang, J.H., Yin, A., Harrison, T.M., Grove, M., Zhang, Y.Q. and Xie, G.H. 2001. A tectonic model for Cenozoic igneous activities in the eastern Indo-Asian collision zone. *Earth and Planetary Science Letters*, **188**, 123–133, https://doi.org/10.1016/S0012-821X(01)00315-6

Wissink, G.K., Hoke, G.D., Garzione, C.N.Jing,L.-Z. and 2016. Temporal and spatial patterns of sediment routing across the southeast margin of the Tibetan Plateau: Insights from detrital zircon. *Tectonics*, **35**, 2538–2563, https://doi.org/10.1002/2016TC004252

Yan, Y., Carter, A., Huang, C.Y., Chan, L.S., Hu, X.Q. and Lan, Q. 2012. Constraints on Cenozoic regional drainage evolution of SW China from the provenance of the Jianchuan Basin. *Geochemistry, Geophysics, Geosystems*, **13**, Q03001, https://doi.org/03010.01029/02011GC003803

Yang, S.Y., Li, C.X. and Yokoyama, K. 2006. Elemental compositions and monazite age patterns of core sediments in the Changjiang Delta: Implications for sediment provenance and development history of the Changjiang River. *Earth and Planetary Science Letters*, **245**, 762–776, https://doi.org/10.1016/j.epsl.2006.03.042

Zhang, Z.J., Tyrrell, S., Li, C.A., Daly, J.S., Sun, X.L. and Li, Q.W. 2014. Pb isotope compositions of detrital K-feldspar grains in the upper–middle Yangtze River system: Implications for sediment provenance and drainage evolution. *Geochemistry, Geophysics, Geosystems*, **15**, 2765–2779, https://doi.org/10.1002/2014GC005391

Zheng, H.B. 2015. Birth of the Yangtze River: age and tectonic–geomorphic implications. *National Science Review*, **2**, 438–453, https://doi.org/10.1093/nsr/nwv063

Zheng, H.B., Clift, P.D., Wang, P., Tada, R., Jia, J.T., He, M.Y. and Jourdan, F. 2013. Pre-Miocene birth of the Yangtze River. *Proceedings of the National Academy of Sciences*, **110**, 7556–7561, https://doi.org/10.1073/pnas.1216241110

Zheng, Y., Jia, J., Nie, X.K. and Kong, P. 2014. Cosmogenic nuclide burial age of the Sanying Formation its implications. *Science China Earth Sciences*, **57**, 1141–1149, https://doi.org/10.1007/s11430-013-4778-z

Zhu, R.X., Potts, R., Pan, Y.X., Lü, L.Q., Yao, H.T., Deng, C.L. and Qin, H.F. 2008. Paleomagnetism of the Yuanmou Basin near the southeastern margin of the Tibetan Plateau and its constraints on late Neogene sedimentation and tectonic rotation. *Earth and Planetary Science Letters*, **272**, 97–104, https://doi.org/10.1016/j.epsl.2008.04.016